Received: 4 January 2017 | Revised: 27 March 2019 | Accepted: 6 April 2019

DOI: 10.1111/jbi.13606

RESEARCH PAPER

Journal of Biogeography | WILEY

Interactions between ecological, evolutionary and environmental processes unveil complex dynamics of insular plant diversity

Juliano Sarmento Cabral[1,2,3] | Kerstin Wiegand[4] | Holger Kreft[2]

[1]Ecosystem Modeling, Center of Computation and Theoretical Biology, University of Würzburg, Würzburg, Germany

[2]Biodiversity, Macroecology & Biogeography, University of Göttingen, Göttingen, Germany

[3]Synthesis Centre of the, German Centre for Integrative Biodiversity Research (iDiv), Leipzig, Germany

[4]Ecosystem Modelling, Büsgen-Institute, University of Göttingen, Göttingen, Germany

Correspondence
Juliano Sarmento Cabral, Ecosystem Modelling, Center for Computational and Theoretical Biology (CCTB), University of Würzburg, am Hubland Nord 32, 97070 Würzburg, Germany.
Email: juliano.sarmento_cabral@uni-wuerzburg.de

Funding information
Ministry of Science and Culture of the State of Lower Saxony, Grant/Award Number: Cluster of Excellence "Functional Biodiversity Research"; Deutsche Forschungsgemeinschaft, Grant/Award Number: FZT 118 and SA 2133/1-1

Editor: Brent Emerson

Abstract

Aims: Understanding how biodiversity emerges and how it varies in space and time requires integration of the underlying processes that affect biodiversity at different levels of ecological organization. We present BioGEEM (BioGeographical Eco-Evolutionary Model), a spatially explicit model that integrates theories and processes understood to drive biodiversity dynamics. We investigated the necessary degree of mechanistic complexity by exploring simulation experiments to evaluate the relative roles of the underlying processes across spatio-temporal scales and ecological levels (e.g. populations, species, communities).

Location: Hypothetical oceanic islands.

Methods: BioGEEM is stochastic and grid-based, and it integrates ecological (metabolic constraints, demography, dispersal and competition), evolutionary (mutation and speciation) and environmental (geo-climatic dynamics) processes. Plants on oceanic islands served as a model system. We ran the simulations both with all processes on and with selected processes switched off to assess the role of each process from the emergent patterns.

Results: The full model was able to generate patterns matching empirical evidence and theoretical expectations. Population sizes were largest on young islands, and species, particularly endemics, better filled their potential range on young and old islands due to limited area and reduced competition. Richness peaked at mid-elevations. The proportion of endemics was highest in old, large and isolated environments within the islands. Species and trait richness showed unimodal temporal trends. Switching off selected processes led to several unrealistic patterns, including the evolution of super-dominant species, extremely high richness and weakened spatial diversity gradients.

Main conclusions: The main predictions derived from BioGEEM are: Competition has cross-scale effects on diversity. Hump-shaped temporal dynamics can be obtained without speciation. Endemic species seem less susceptible to extinction than native non-endemic species. Endemism reflects stronger geographical and environmental isolation. Finally, only the integration of all implemented processes generates realistic spatio-temporal dynamics at population, species, community and assemblage levels.

KEYWORDS
demography, dispersal, interspecific competition, island biogeography, mechanistic simulation model, metabolic theory, plant community, process-based niche model, speciation, species richness

1 | INTRODUCTION

Ecologists and biogeographers have a long-standing interest in explaining how species are distributed in space and time, but disentangling the role of various mechanisms for the generation and maintenance of biodiversity remains a challenge (e.g. Hurlbert & Stegen, 2014; Pontarp et al., 2019). To advance our understanding of diversity patterns, it has been suggested that it is crucial to account for the interplay between eco-evolutionary processes and environmental dynamics (Cabral, Valente, & Hartig, 2017; Pontarp et al., 2019; Urban et al., 2016). Some mechanistic models simulate eco-evolutionary processes at the species and/or community ecological levels (e.g. colonization, speciation, extinction) to generate biogeographical patterns of interest (e.g. Colwell & Rangel, 2010; Gotelli et al., 2009). Other models simulate processes at lower ecological levels, such as propagule dispersal and population establishment (e.g. Harfoot et al., 2014; Urban et al., 2016). Such low-level models are not necessarily more complex in terms of number of parameters than high-level models, but have the advantage to generate both low- and high-level patterns. Hence, typical biogeographical processes (e.g. colonization and extinction) become emergent rather than imposed (Leidinger & Cabral, 2017). This provides insights across ecological levels (Harfoot et al., 2014; Rosindell & Harmon, 2013; Urban et al., 2016) and integrates ecological and biogeographical theories by linking low- with high-level processes (Cabral et al., 2017; Leidinger & Cabral, 2017).

A major challenge of integrating multiple processes is the increase in model complexity possibly hampering interpretability due to the risk of 'equifinality', that is, different parameter value combinations resulting in similar outcomes (Dormann et al., 2012). Existing biodiversity models simulate several mechanisms, but these mechanisms are rarely integrated in a single model (but see Harfoot et al., 2014; Rangel et al., 2018; Urban et al., 2016). This lack of process integration avoids equifinality but also prevents progress on complex phenomena (Cabral et al., 2017). Equifinality can be dealt with by investigating emergent patterns at different scales, that is, pattern-oriented modelling (Grimm & Railsback, 2012). Pattern-oriented models distinguish the effects of different combinations of parameter values that generate similar patterns at a given scale by evaluating patterns at other scales. For this, low-level models are ideal because they generate patterns at multiple ecological levels (Cabral et al., 2017; Leidinger & Cabral, 2017). Likewise, a useful study system should be simple, but still informative across different scales and ecological levels, such as oceanic islands (Leidinger & Cabral, 2017; Losos & Ricklefs, 2010; Warren et al., 2015). In fact, island research has made important contributions to our understanding of eco-evolutionary processes shaping biodiversity (e.g. Ricklefs & Bermingham, 2004; Whittaker & Fernández-Palacios, 2007), including theoretical frameworks and models (e.g. Darwin, 1859; MacArthur & Wilson, 1963; Whittaker, Triantis, & Ladle, 2008).

To model insular biodiversity, it is necessary to integrate the processes driving biodiversity in general with the processes shaping island diversity in particular. Local population dynamics, individual dispersal, biotic interactions and metabolic constraints are four essential processes for biodiversity dynamics (Harfoot et al., 2014; Urban et al., 2016). These processes can be hierarchically integrated: dispersal connects local populations while metabolic constraints control demographic transitions and resource competition (Cabral et al., 2017). Dispersal between populations reflects a metapopulation framework (Hanski, 1999), where local population dynamics and short- and long-distance individual dispersal are explicitly simulated (Cabral & Schurr, 2010). Intra- and interspecific competition are central to modern coexistence theories (e.g. Chesson, 2000) and can be implemented in species-rich communities via interaction currencies (Kissling et al., 2012). The metabolic theory of ecology provides constraints that are applicable to resource depletion scenarios (Savage, Gillooly, Brown, West, & Charnov, 2004) and to all organisms, with higher temperature and smaller body mass increasing all biological rates (Brown, Gillooly, Allen, Savage, & West, 2004). Integrating these mechanisms within a niche-based framework can generate realistic patterns for species and communities along elevational gradients (Cabral & Kreft, 2012). Adding environmental and evolutionary processes ultimately completes the minimum set of processes necessary for biodiversity dynamics (Cabral et al., 2017; Urban et al., 2016). For hotspot oceanic islands, simplified geological ontogenies have been inferred, namely humped trajectories of area, elevation and environmental heterogeneity (Whittaker & Fernández-Palacios, 2007). This ontogeny is the basis of the General Dynamic Model (GDM) of oceanic island biogeography (Whittaker et al., 2008) and provides the necessary environmental processes. Finally, gene flow from the mainland limiting insular differentiation as well as mutations that can trigger within-island radiation provide the microevolutionary processes for insular macroevolutionary dynamics (Rosindell & Phillimore, 2011). The emergent patterns resulting from a model integrating all these processes should encompass patterns at lower ecological levels (e.g. rank-abundance distributions; Rosindell & Harmon, 2013) and high-level patterns (e.g. biogeographical rates).

In this modelling study, we investigate the role of ecological, evolutionary and environmental processes for biodiversity dynamics and present a process-based BioGeographical Eco-Evolutionary Model (BioGEEM). Extending a previous population-based, niche-based

simulation model (Cabral & Kreft, 2012), BioGEEM was developed to include evolutionary and environmental processes. Here we focus on an idealized oceanic hotspot island as a model system. We first used the full model to assess emergent patterns across four ecological levels (populations, species, local communities, island assemblage) against theoretical predictions and empirical patterns. We then assessed whether the proposed complexity is necessary by switching off key processes (competition, metabolic constraints, environmental dynamics, speciation) and re-evaluating emergent patterns. The fact that the various emergent patterns remained realistic only with all implemented mechanisms demonstrates the cross-level generality of integrating basic principles of ecological and evolutionary processes.

2 | MATERIALS AND METHODS

2.1 | General model description

We extended a previous niche-based, spatially explicit multispecies simulation model for range dynamics of plants (Cabral & Kreft, 2012; for details see Appendix S1) and added evolutionary and environmental processes within a theoretically based hierarchical framework (Figure 1a; see also Figure S1 of Appendix S2). The model was written in C++ with imbedded Matlab code (Armadillo library – Sanderson & Curtin, 2016), implemented in Visual Studio 2010. The code is publicly available at https://github.com/julianoscabral/BioGEEM. Outputs were analysed in R (R Core Team, 2018).

In the model's hierarchical framework, body mass and local temperature determined demographic transitions (germination, sexual maturation, reproduction and density-independent mortality), mutation rates (important for within-island radiation), the space exploited by an individual, population carrying capacity and time for speciation. We simulated two types of speciation: mainland-island differentiation and within-island radiation. These processes relate to anagenetic and cladogenetic speciation sensu Stuessy et al. (2006), but are better described by their geography as regionally allopatric and regionally sympatric speciation, respectively (see a terminology review in Emerson & Patino, 2018a; see also Meiri, Raia, & Santos, 2018 and Emerson & Patino, 2018b). In BioGEEM, mainland-island differentiation is neutral and non-adaptive, whereas within-island radiation is non-neutral and adaptive (i.e. niche evolution). For simplicity, we refer to species emerging from the simulated mainland-island differentiation and from within-island radiation as 'differentiated endemics' and 'radiated endemics', respectively. Metabolic constraints decreased biological rates (e.g. metabolic, demographic, evolutionary) and increased biological times (e.g. speciation time) with body mass while increasing rates and decreasing times with temperature (Brown et al., 2004; Savage et al., 2004). Metabolic constraints further accounted for trade-offs related to energy allocation (e.g. survival vs. growth). We focused on terrestrial seed plants, but these metabolic constraints are ubiquitous (Brown et al., 2004). Below, we summarize the model, with a detailed description following the Overview, Design concepts and Details protocol (ODD, Grimm et al., 2010) in Appendix S1.

2.2 | State variables and scales

The model is grid-based with grid cells being 1 km^2 in size. The grid dynamics reflected geomorphological phases of oceanic islands (Figure 1b,c; Whittaker & Fernández-Palacios, 2007; Whittaker et al., 2008). Each island cell was assigned to a side (north, east, south, west) and to an elevation with an associated temperature. Diagonal cells represented ecotones, belonging to two island sides (all four for the central cell). The model agents were stage-structured populations (seeds, juveniles, adults). Populations belonged to species, which were characterized by 11 autecological properties: maximum cell suitability, optimum temperature, temperature amplitude, optimum island side, island side amplitude, life form (herb, shrub, or tree), mean dispersal distance, dispersal kernel thinness, strength of Allee effects, stage-specific body masses and phenological ordering related to entire species pool. Optimum island side and island side amplitude were added to BioGEEM to add environmental heterogeneity beyond temperature, such as precipitation. Indeed, islands have strong windward/leeward precipitation differences (Whittaker & Fernández-Palacios, 2007). Environmental heterogeneity was created by island sides and temperature gradients and changed over time due to island geodynamics, with maximum heterogeneity occurring at maximum island size. Environmental heterogeneity was used to calculate species' habitat suitability, which influenced germination and reproduction and thus defined both establishment and persistence niches. The mean dispersal distance and the dispersal kernel shape parameter described short- and long-distance dispersal, respectively, following Clark's 2Dt dispersal kernel (Clark, Silman, Kern, Macklin, & HilleRisLambers, 1999; Nathan & Muller-Landau, 2000), allowing both within-island and mainland-island dispersal.

Cell area was used as the interaction currency (Kissling et al., 2012): an individual exploited a certain physical space, which was defined by the individual's body mass and influenced by local temperature (Savage et al., 2004). A cell could only hold a single population per species, but could hold many species as long as there was area available. Hence, species coexistence in a cell and on the island was not imposed (monodominance possible and no zero-sum assumption) but emerged from stochastic transitions (e.g. mortality) and local competition for area (Cabral & Kreft, 2012). The fact that metabolic constraints on carrying capacity modulated local competition meant that metabolic constraints constituted a coexistence mechanism.

The state variables comprised the spatial distribution of seed, juvenile and adult abundances of each species and the unoccupied area. Each time step was 1 year and a complete simulation ran for 2.21 million time steps (Figure 1d). Eco-evolutionary processes took place every time step, whereas environmental events happened at longer intervals (Figure 1e).

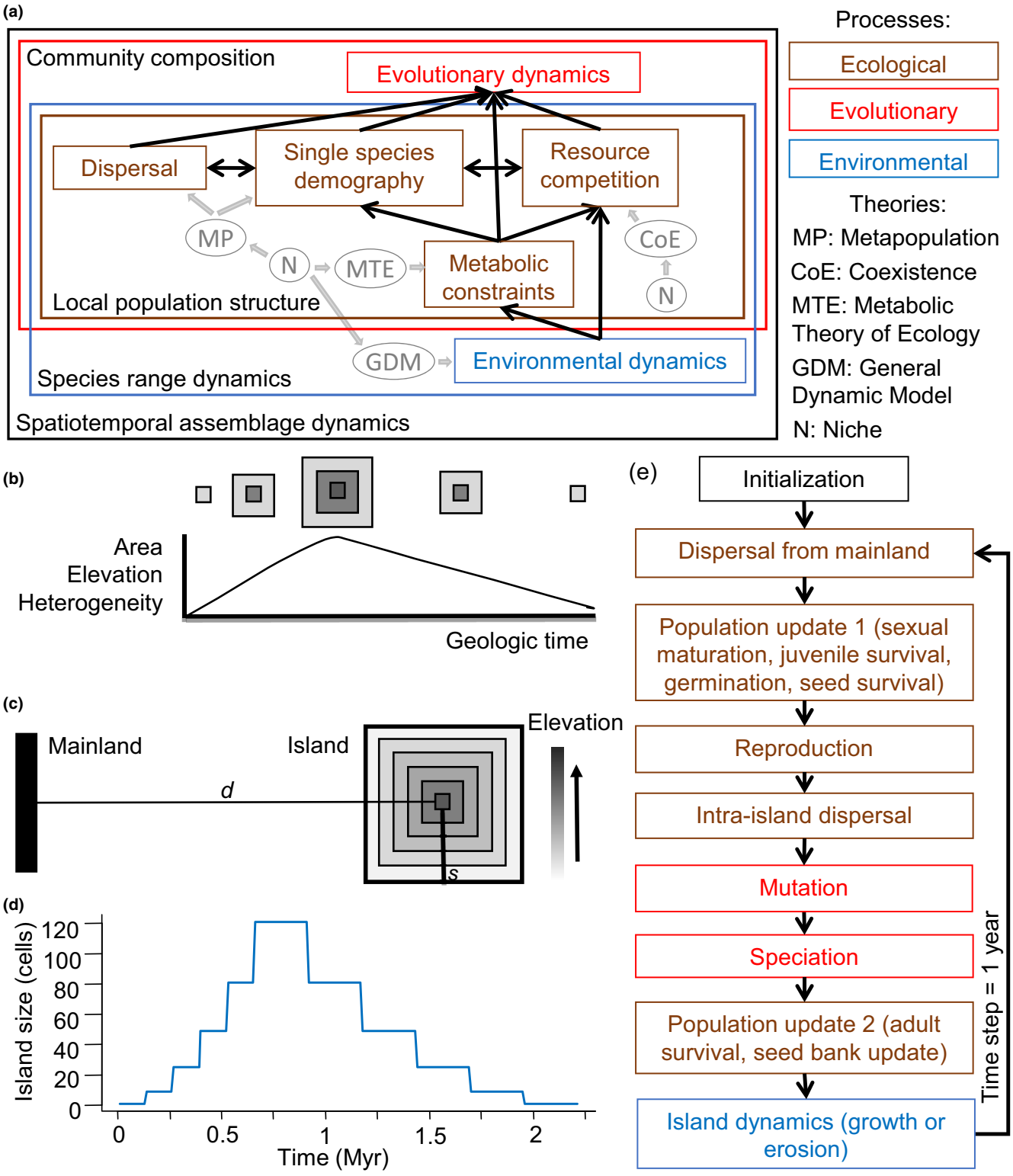

FIGURE 1 Model framework. (a) Hierarchical structure of simulated processes, emergent patterns and integrated theories. (b) Growth and erosion of hypothetical volcanic islands over geological time. Elevation and environmental heterogeneity are expected to correlate positively with island size and thus to be a humped function of island age. (c) Simulation grid at maximum island size, where *s* is the maximum distance between island centre and edge (*s* = 5 cells). Grid dimensions are described by *s* and distance *d* from the island centre to the mainland: (2*s* + 3) (*s* + *d*+4) cells. The island initially starts as a single cell at *s* + 1 cells from the right, top and bottom borders of the grid and the mainland is at the left grid margin with two columns of cells. (d) Island size over time, with each simulation spanning 2.21 Ma. (e) Flow chart illustrating the sequence of simulated processes. Note that ecological and evolutionary processes were performed every time step, but island dynamics took place at much greater intervals (d)

2.3 | Initialization

The model was initialized by reading in the simulation grid (Figure 1c) and the run specifications: mean annual air temperature at sea level (298 K, or 25°C), species pool size (1,000 species) and intervals for randomly drawing the species properties. Each species received random properties, from which its habitat suitability matrix on the island, $\boldsymbol{H}$, and its dispersal kernel, $\boldsymbol{D}$, were calculated. The abundance matrices for adults, $\boldsymbol{N_a}$, juveniles, $\boldsymbol{N_y}$, and seeds, $\boldsymbol{N_s}$, of each species and the matrix with the occupied area, $\boldsymbol{A_t}$, were initialized empty.

2.4 | Dispersal from mainland

At each time step, 10 random species dispersed from each mainland cell f to the island (mainland dimensions in Figure 1c). Dispersal from the mainland did not imply effective colonization, as not all species could reach the island and germination happened only in suitable cells (for variation in the number of dispersing species, see Cabral, Whittaker, Wiegand, & Kreft, 2019). The seed bank for each species was incremented by Poisson $\left(\sum_f D_{(i,f)}\,\text{Uniform}(1,10000)\right)$, where $D_{(i,f)}$ was the per-seed dispersal probability from cell f to cell i and the upper distribution boundary reflected the maximum number of the largest adults (Appendix S1).

2.5 | Population update 1

Following the phenological order, abundances were sequentially updated by: (a) turning juveniles to adults, (b) applying density-independent mortality to remaining juveniles, (c) germinating seeds and (d) applying seed mortality. If germinating and maturing individuals surpassed the available space, excess individuals died from self-thinning (Wiegand, Saltz, Ward, & Levin, 2008).

2.6 | Reproduction

The number of seeds produced by species j in cell i ($S_{p(i,j)}$) was given by $N_{a(i,j)}\,R(N_{a(i,j)})$, where $N_{a(i,j)}$ was the number of adults of species j in cell i and R a function for density-dependent reproduction.

2.7 | Intra-island dispersal

Seeds of species j received in cell z and from source cell i, ($S_{d(z,j)}$), were given by $\sum_i D_{(z,i)}S_{p(i,j)}$.

2.8 | Mutation and niche evolution

We implemented a point-mutation process as a simple yet efficient way to model within-island radiation (i.e. speciation where two or more species evolve from a common ancestor, Rosindell & Phillimore, 2011). The number of mutated seeds was a Poisson random variable, whose probability (i.e. Poisson's λ) was given by multiplying $S_{d(z,j)}$ with a metabolic mutation rate. These individuals were initialized with random maximum cell suitability, optimum temperature, temperature amplitude, optimum island side and island side amplitude (see Section 2.3). The remaining species properties were randomly drawn from within the ±50% intervals around the ancestral values. This phylogenetic constraint was arbitrary but kept the phylogenetic trait structure while allowing for the considerable divergence that is often found on islands (Whittaker & Fernández-Palacios, 2007). Phylogenetic constraints were not varied, but we expect that increasing constraints would cause stronger competition between incipient species, thus decreasing their survival, speciation rate and trait divergence. The evolving properties allowed for functional and adaptive divergence, as all species properties were functional. Real-world spatial and attribute divergence can also be driven by non-adaptive processes (e.g. isolation of populations followed by neutral mutations). Non-adaptive, neutral differentiation happened only between island colonizers and the mainland source pool, driven by isolation and limitations to gene flow. Implementing neutral mutations was beyond our scope and would increase mechanistic complexity (e.g. by including neutral mutable properties, intra-island barriers and/or population genetics), but we expect this would increase radiations (i.e. by adding non-adaptive radiations).

2.9 | Speciation

We checked whether the time for diverging individuals to become a distinct species was reached for both types of simulated speciation, namely mainland-island differentiation and within-island radiation ('protracted speciation' – Rosindell & Phillimore, 2011). Mainland-island differentiation was a neutral process, that is, island colonizers became distinct from the mainland form without changing their properties. Both speciation types depended on metabolic constraints to account for longer generations for larger body mass (Brown et al., 2004). For mainland-island differentiation, the speciation time was counted from the island colonization event. However, later colonizers delayed mainland-island differentiation due to gene flow. The delay was arbitrary but varied metabolically and could prevent mainland-island differentiation. For within-island radiation, the speciation time was counted from the time step of the mutation.

2.10 | Population update 2

Abundance matrices were updated sequentially by applying density-independent mortality to adults and updating the seed bank.

2.11 | Environmental dynamics

We considered the simplified geo-climatic dynamics of an idealized oceanic hotspot island (Figure 1b; sensu Whittaker & Fernández-Palacios, 2007). To mimic volcanic island growth, each simulation started with a single cell that grew regularly by adding concentric belts of cells around the margins and uplifting the interior belts. Thereafter, island size remained temporarily stable, followed by an erosion phase. At each erosion step, one belt of cells disappeared

from the island margin and the elevation of remaining cells decreased (Figure 1b). Temperature decreased by 1 K for each elevational belt following uplift and increased by 1 K following erosion. We assumed an arbitrary growth time step of 0.13 Ma (based on Madeira island in Portugal – Appendix S1). We doubled this time length for the stable and erosion phases to account for slower geodynamics (Whittaker & Fernández-Palacios, 2007). After every environmental event, ***H*** was recalculated for every species. This temporal framework was arbitrary and hotspot island trajectories describe only some systems, but exploratory experiments varying environmental dynamics showed qualitatively similar trends (see Figure S2 of Appendix S2 for faster environmental dynamics, larger maximum island area and simulations without changes in habitat heterogeneity) and varying the geological trajectories has been assessed elsewhere (Borregaard, Matthews, & Whittaker, 2016).

2.12 | Output

Output variables were N_a, N_y and N_s. Additionally, we recorded time series of species richness (total, non-endemics, differentiated and radiated endemics), radiating lineages (colonizing lineages showing within-island radiation), species per radiating lineage, colonization, speciation and extinction events.

2.13 | Study design

We designed two simulation experiments. First, we simulated the full model, assessed multiple patterns across ecological levels (for model generality; Evans et al., 2013) and compared them to empirical data and theoretical predictions whenever possible (to deal with equifinality; Dormann et al., 2012). The maximum island size was 11 × 11 cells and the mainland species pool comprised 1,000 species. Although this maximum size is comparatively small for oceanic islands with high endemism (Kisel & Barraclough, 2010), it allowed us to investigate endemism while retaining computational feasibility. At maximum size, the simulated islands were 300 cells away from the mainland. To account for variability of emergent patterns, we simulated 20 replicate runs, each with a different mainland source pool (Figure S3 of Appendix S2).

In the second experiment, we switched off the processes to assess their relative role. Three replicate model runs were performed for each scenario. This number of replicates already captured the temporal trends in variability (Figure S3 of Appendix S2), while still allowing us to explore highly computationally demanding scenarios. We simulated four scenarios: without competition, without metabolic constraints, without environmental dynamics and without speciation. Except for the scenario without metabolic constraints, replicate runs were based on the same source pool, thereby controlling for source pool-related variability. For the scenario without competition, we simulated each of 500 random species from the source pool alone. However, competition still took place between evolving species. Otherwise, endemic richness would have been unrealistic, that is, increased exponentially. For the scenario without metabolic constraints, we switched off the body mass and local temperature control on demographic and evolutionary rates, which were then drawn independently (e.g. no trade-offs between demographic rates). For the scenario without environmental dynamics, the island had a constant size of 7 × 7 cells. For the scenario without speciation, we switched off gene flow, mutation, mainland-island differentiation and within-island radiation. Given our focus on general trends emerging from models simulating explicit causal relationships, we depicted averages across replicates (with 95% confidence envelopes). We did not perform statistical tests because significance tests are less relevant for mechanistic simulation experiments as spurious differences emerge by simply increasing replication (Murray & Corner, 2009; White, Rassweiler, Samhouri, Stier, & White, 2014).

3 | RESULTS

The first experiment generated temporally and spatially explicit patterns over levels of ecological organization. At the population level, population structure and abundances at local to whole-island scale were highly dynamic and variable (Figure 2a–f). Population structure (proportion of seeds, juveniles and adults) varied from mostly stable within some environmental steps (Figure 2b,d,f) to ever changing (Figure 2a,e). Non-endemic species decreased in mean abundance (Figure 2g), whereas insular endemics derived from differentiation from mainland populations (Figure 2h) and derived from within-island radiation (Figure 2i) had more stable adult abundances and even increased at later stages.

At the species level, the spatial distribution of abundance and realized range changed over time and could strongly deviate from the distribution of potential habitat, with some species surviving only in suboptimal environments (Figure 3a). Species tended to have lower range filling at intermediate to advanced island age, with radiated endemics retaining higher values than differentiated endemics and non-endemics (Figure 3b).

At the community level, rank-abundance distributions followed a lognormal distribution (Figure 4a). Local species richness, richness of radiated endemics, proportion of radiated endemics, proportion of all endemics and number of species per radiating lineage increased over time (Figure 4b–f). Species richness and radiated endemic richness peaked at intermediate elevations when the island reached maximum size (Figure 4b,c). The proportions of all endemics and of radiated endemics were highest at low elevations (Figure 4d,e). Trait composition also changed over time, with increasing adult biomass at higher elevations (Figure 4g) and decreasing long-distance dispersal at low elevations (Figure 4h).

At the level of the island-wide assemblage, species–area relationships (SARs) were steeper during the growth phase than during the erosion phase (Figure 5a,b). Species richness showed a humped trend and peaked at intermediate to advanced age (Figure 5c), whereas both types of endemics peaked slightly later (Figure 5c). The proportion of endemics generally increased over time, except for a weak very late hump for radiated endemics (Figure 5d).

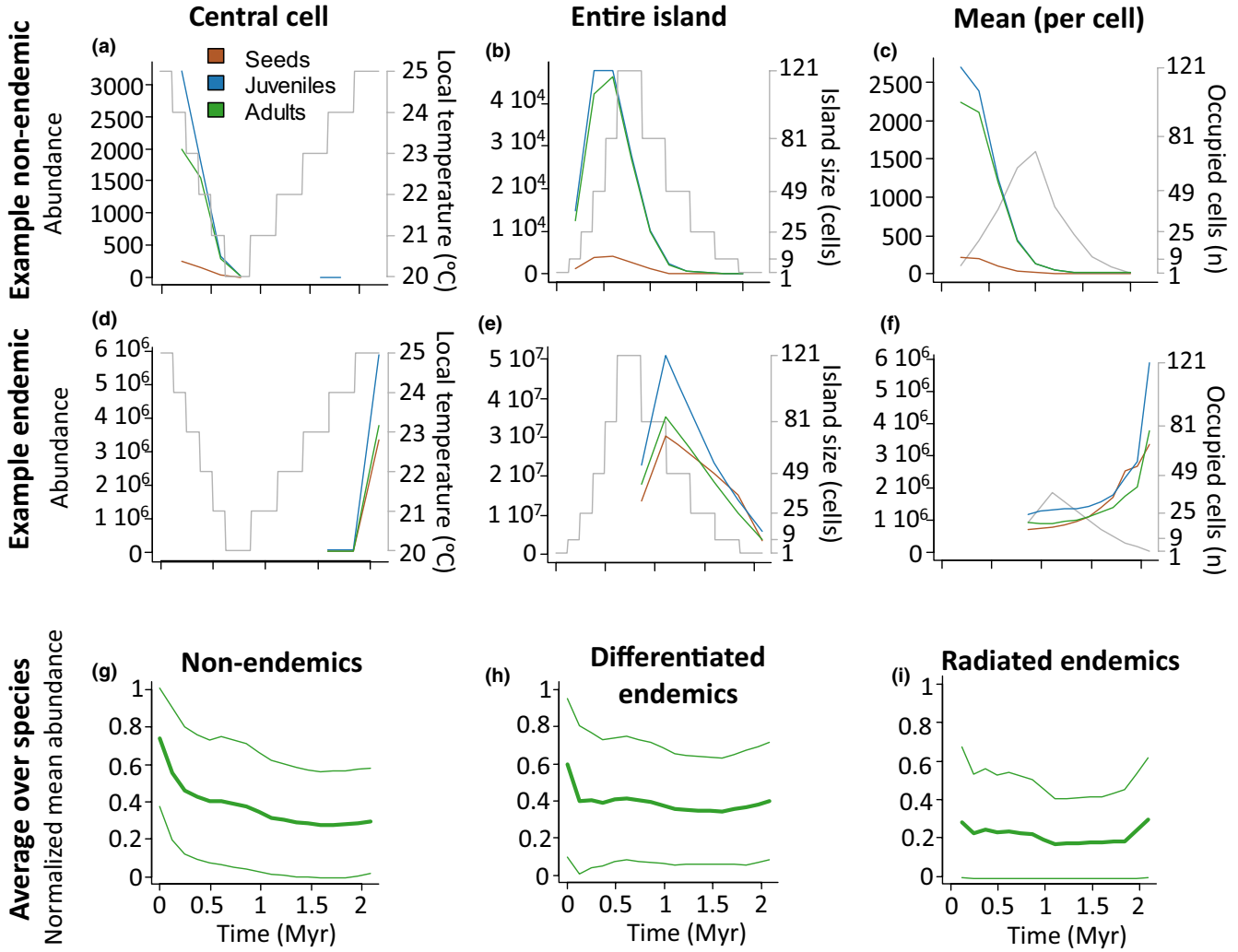

FIGURE 2 Population level temporal patterns. The top and intermediate rows show one exemplary species each, whereas the bottom row describes the abundance of adults normalized by dividing the time series by the maximum abundance. (a–c) Seed, juvenile and adult abundances (a) in number of individuals of a non-endemic tree species adapted to lowlands and (d–f) of an endemic herb species adapted to lowlands (detailed species properties in Appendix S1). Panels (a) and (d) give local abundances in the central cell, (b) and (e) total island abundances and (c) and (f) mean abundances (per occupied cell). The grey lines in (a–f) refer to the right *y*-axis: local temperature of the central cell (a, d), number of island grid cells (b, e) and occupied island grid cells (c, f). (g–i) Normalized mean cell abundances of (g) non-endemics, (h) differentiated endemics and (i) radiated endemics. Mean cell adult abundances were normalized by the highest value in the time series per species. Thick lines in (g–i) indicated the average over replicates (n = 20) and species, whereas thin lines indicate 95% CI (truncated at 0 and 1). All time series were further averaged within each geological time step

Colonization and extinction rates were humped and peaked at intermediate island ages, with a later second minor peak for extinction (Figure 5e). The rates of both speciation types also had a humped trend (Figure 5f). Extinction of endemics was humped with a late peak (Figure 5f). The average number of radiating lineages and the number of species per radiating lineage peaked at advanced island ages (Figure 5g). However, the dynamics of the number of species per radiating lineage largely varied between and within replicates (Figure 5h–i), with lineages showing constant increases, hump-shaped trends or saturating species numbers. Taxon cycles also emerged in some replicates, with early diversifying lineages being replaced by later diversifying lineages (Figure 5i). Trait richness was humped over time (Figure 5j), but species packing showed an initial steep decrease followed by a humped temporal trend (Figure 5k). For the radiated endemics, the mean pairwise trait distance to their ancestral species showed a very shallow humped temporal trend, whereas the distance to all species increased almost for the entire island lifespan, decreasing only at very advanced island age (Figure 5l).

Scenarios with selected processes switched off revealed patterns diverging from the full model (Figure 6). At the population level, population size and structure were generally stable within environmental steps in the scenarios without competition (Figure 6a vs. inset in Figure 6c) and metabolic constraints (Figure 6b), although the latter could reach much higher sizes. Without environmental dynamics, species colonized earlier, but could go extinct as in the full model

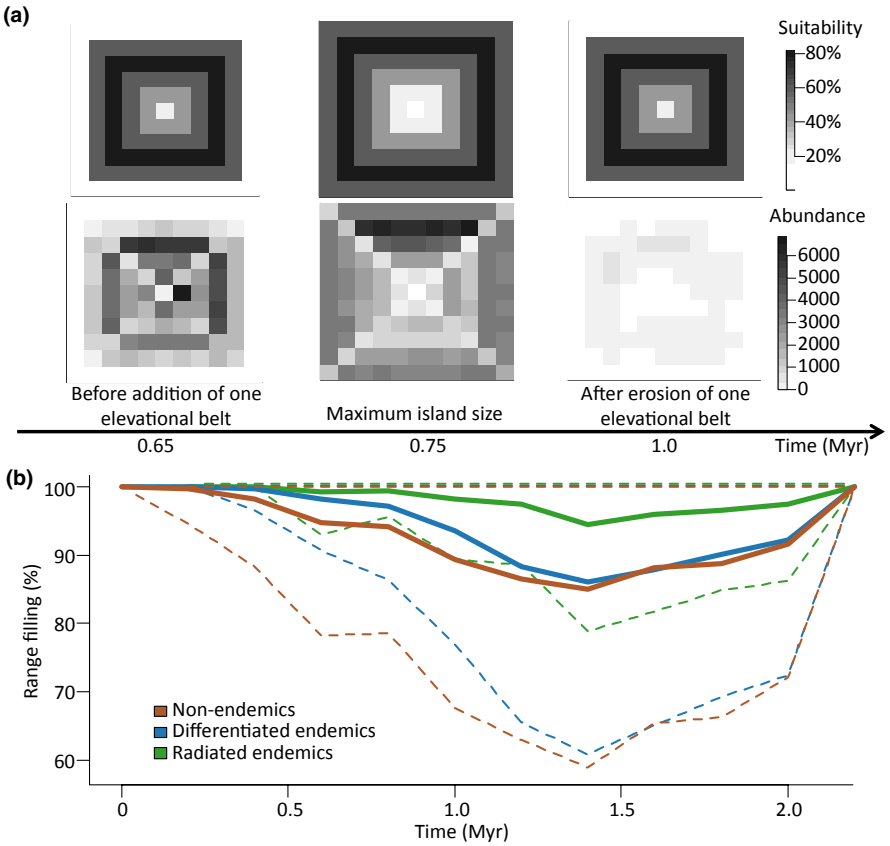

FIGURE 3 Temporal and spatial patterns at the species level. (a) Potential (top row) and realized (bottom row) range of a shrub species adapted to lowlands (T_o = 24°C, T_a = 4) at three different time steps: before (left column), during (middle column) and after (right column) the island has reached maximum size (species properties in Appendix S1). (b) Range filling time series of non-endemic species, differentiated endemics and radiated endemics (n = 20; thick lines indicate means, thin dashed lines 95% CI). Time series in (b) were averaged within each geological time step

(Figure 6c). Without speciation, colonizers decreased in abundances over time, but survived over the entire simulation period (Figure 6d). At the species level, range filling was lower at intermediate island age and for radiated endemics without competition (Figure 6e vs. inset in Figure 6g), whereas without metabolic constraints, range filling was variable, with non-endemics going extinct (Figure 6f). Without environmental dynamics, range filling was highest for radiated endemics, but showed stable dynamics after the initial colonization period (Figure 6g). Without speciation, species maintained high levels of range filling (Figure 6h). At the community level, the proportion of radiated endemics was extremely high at advanced island age without competition, particularly in the lowlands (Figure 6i vs. inset in Figure 6l). In the scenario without metabolic constraints, the proportion of radiated endemics was also high, but without spatial structure (Figure 6j). Moreover, without environmental dynamics, the proportion of radiated endemics peaked at low and high elevations (Figure 6k), whereas endemics were logically absent without speciation (Figure 6l). At the assemblage level, species richness showed a humped temporal trend dominated by endemics, with very high values without competition (Figure 6m vs. inset in Figure 6p) and very low values without metabolic constraints (Figure 6n). Without environmental dynamics, total species richness tended towards equilibrium but the number of radiated endemics increased steadily (Figure 6o). Without speciation, species richness showed a humped trend similar to, but with lower values and less variation than, the full model (Figure 6p).

4 | DISCUSSION

4.1 | Population level

In the full model, population structure varied according to local environmental conditions, evolutionary origin (non-endemic, differentiated or radiated) and island age (Figure 2). The high relative abundances on young islands (particularly of non-endemics, Figure 2g) coincided with low species numbers (Figure 5c) and, thus, might reflect lower competition. Indeed, without competition, species sustained high and stable abundances throughout the simulation period (Figure 6a), whereas without speciation (i.e. without competition with endemics), abundances decreased over time, but populations still survived longer than in the full model (Figure 6d). Lower population establishment on older islands has also been observed for biological invasions on islands worldwide (Kueffer et al., 2010). Accordingly, endemics sustained more stable populations compared to non-endemics (Figure 2g–i). Empirical data comparing abundances of endemic and non-endemic plant species are rare, but pollination networks on oceanic islands suggest that endemics tend to be generalists and have higher relative abundances than non-endemics (Olesen, Eskildsen, & Venkatasamy, 2002). Future modelling studies may change the source pool to mimic Late Quaternary glacial cycles (e.g. Weigelt, Steinbauer, Cabral, & Kreft, 2016) or to include human-mediated biological invasions, which are particularly prevalent on oceanic islands and which may easily outcompete endemic species. Moreover, other types of interactions (e.g. trophic,

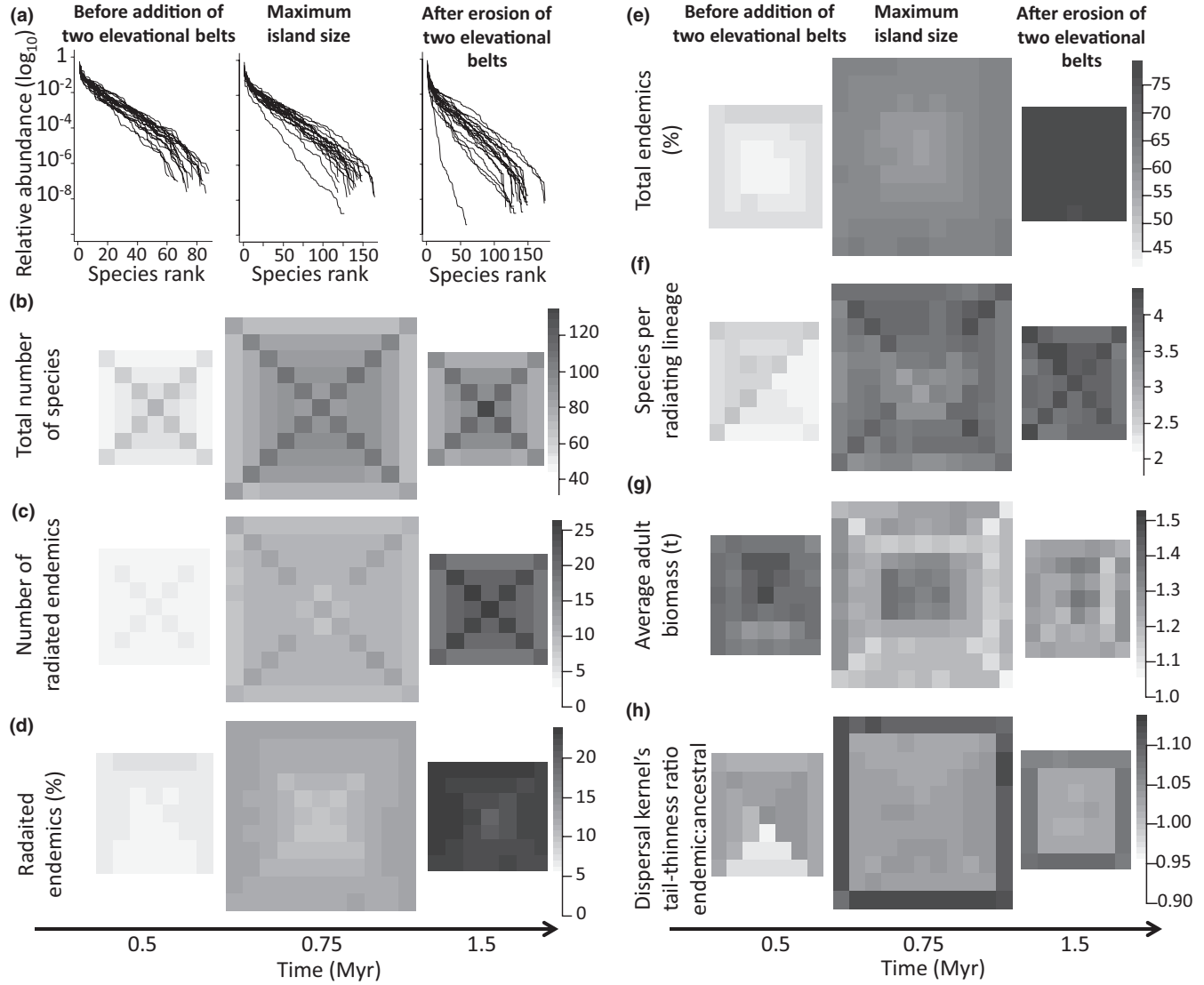

FIGURE 4 Temporal and spatial patterns at the community level. (a) Rank-abundance plots of the central cell. Spatially explicit (b) total number of species, (c) number of radiated endemics, (d) proportion of radiated endemics, (e) proportion of all endemics, (f) number of species per radiating lineage, (g) adult biomass averaged over co-occurring species and (h) ratio between the dispersal kernel's tail-thinness of radiated endemics and that of their ancestral island colonizer averaged across co-occurring endemics, all of these at three different times steps: before (left panels), during (middle panels) and after (right panels) the island has reached maximum size. Rank abundances of each replicate are given by single lines in (a) and all of them fitted the lognormal distribution best when comparing AIC values for fitted logseries, lognormal and power law distributions to the abundance data (R package 'sads'). (b–h) Averaged over the 20 replicate runs and illustrate the diversity of emergent local patterns across space and time. Note an increase in biomass towards highlands (g) and a selection towards lower long-distance dispersal ability (higher kernel's tail-thinness) over time, particularly at the island edges (h)

mutualistic) could be integrated to test whether generalism is indeed selected. Nevertheless, current results already indicate that competition regulates populations by decreasing abundances over time, supressing establishment of colonizers and selecting for strongly competitive endemics.

4.2 | Species level

Under the full model experiment, the decrease in abundances discussed above translated into a decrease in species' range filling at intermediate to advanced island ages (Figure 3). Even if species filled their entire potential range, the spatial abundance distribution could diverge from the distribution of habitat suitability (Figure 3a). Such divergence can be explained by interspecific competition, which may shift abundances to suboptimal environmental conditions (Cabral & Kreft, 2012), as reported for plants and animals (McGill, 2012; Wisz et al., 2013). With decreasing island size, extinction of poorer competitors increased range filling of surviving species (Figure 3b). Radiated endemics better filled their potential range compared to non-endemics and differentiated endemics (also when comparing species with different preferred elevations – Figure S4 of Appendix S2), which indicates

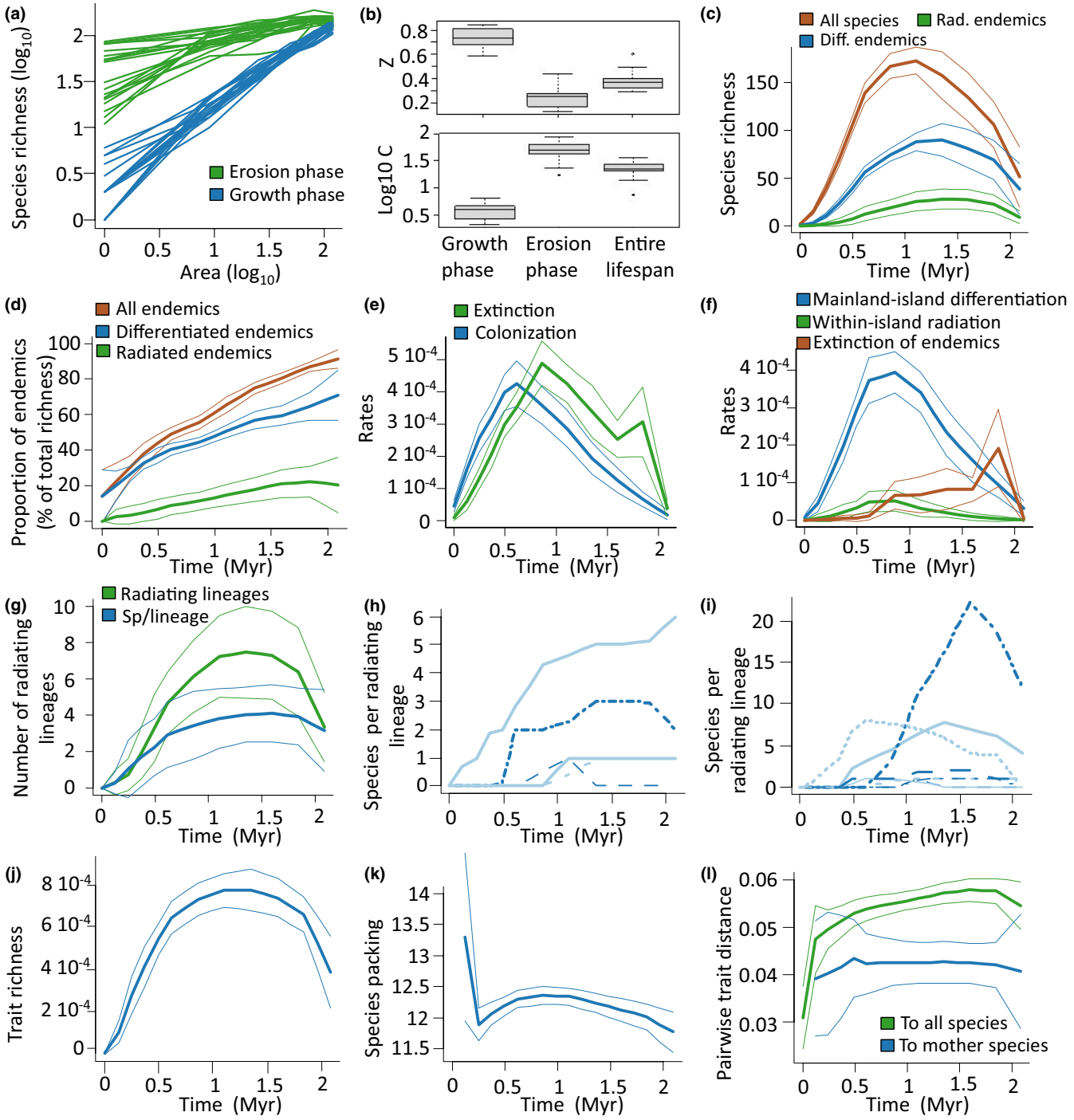

FIGURE 5 Temporal patterns at the assemblage level. (a) Log–log species–area relationships (SARs) for growth and erosion phases (lines represent replicates), (b) slope *z* and intercept $\log_{10} C$ of estimated power-law SARs for growth and erosion phases as well as the entire island geological lifespan, (c) species richness over time, (d) proportion of endemic species compared to total richness over time, (f) colonization and extinction rates over time, (f) mainland-island differentiation, within-island radiation and extinction rates of endemics over time, (g) number of radiating lineages and species per radiating lineage over time, (h–i) species per radiating lineage (each line is a lineage) in three replicate runs showing great variability in time series shapes (unimodal, saturating, increasing trends), (j) trait richness (volume of the convex hull of the multivariate space considering all species properties) over time, (k) species packing (number of species per trait richness unit) over time, (l) pairwise trait distance of radiated endemics to their mother species and to all other species over time, averaged per trait and per species pair. Rad. and Diff. in the legend in (c) mean radiated and differentiated, respectively. Lines in (c–l) indicate values averaged within each environmental time step, further averaged over 20 replicates in (c–g; j–l) with 95% CI thin lines

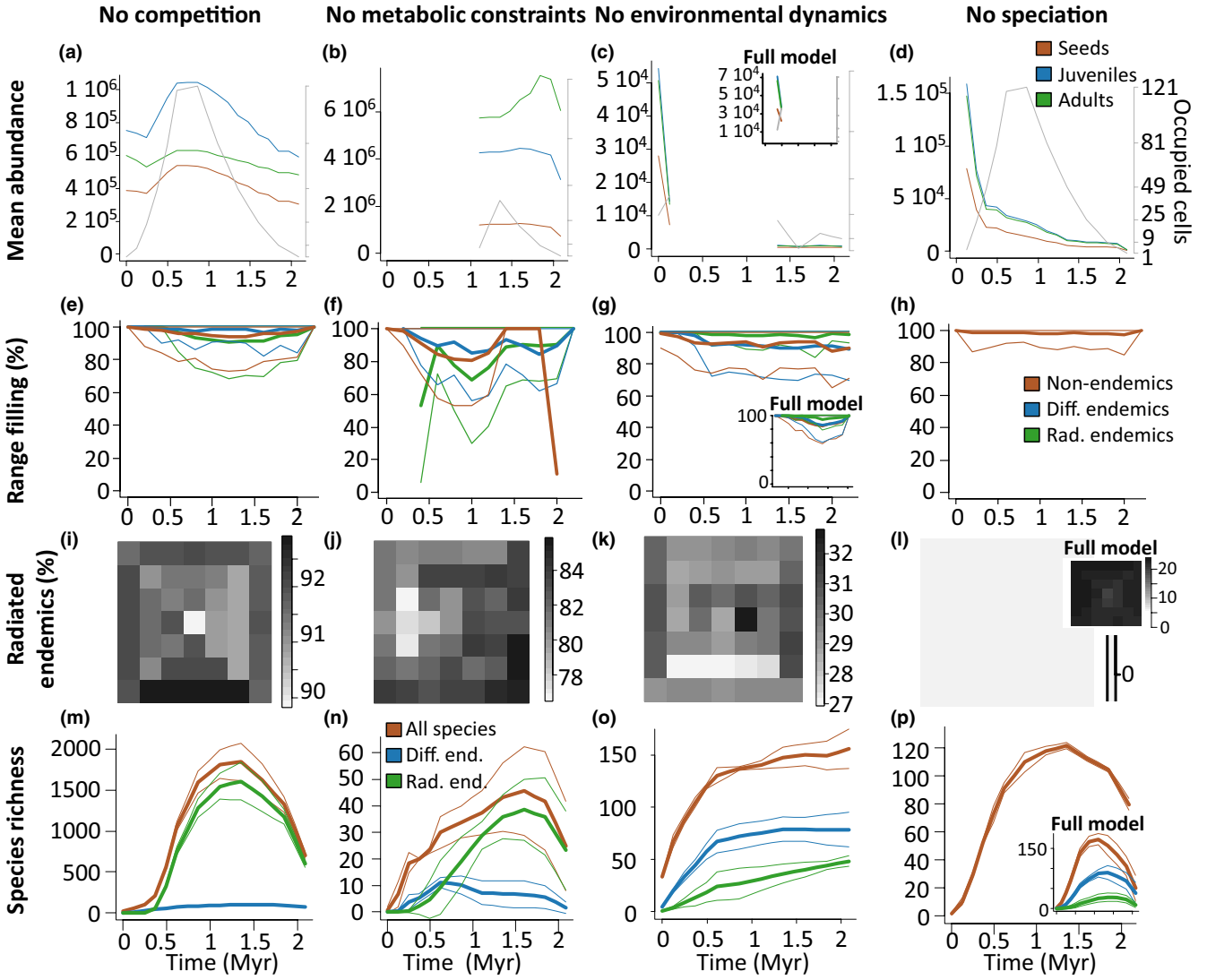

FIGURE 6 Evaluation of the model structure across patterns at different ecological levels (rows) by switching off key processes (columns). (a–d) Population dynamics of an example species, given by mean abundances (per occupied cell). (e–h) Overall range filling dynamics. (i–l) Proportion of radiated endemics at advanced island age, 1.5 Ma. (m–p) Total species richness dynamics of exploratory scenarios with no competition (left column), no metabolic constraints (middle left column), no environmental dynamics (middle right column) and no speciation (right column). Colour legends differ between rows: legends in (d) for population dynamics, in (h) for range filling dynamics and in (n) for total richness dynamics (Rad. and Diff. mean radiated and differentiated, respectively). (a), (c) and (d) Illustrate the population dynamics of one example non-endemic shrub species adapted to intermediate elevations that survived in these three scenarios and in the full model (inset in c). (b) The population dynamics of one example radiated endemic herb species adapted to lowlands (species properties in Appendix S1). Grey lines and right *y*-axis in (a–d) indicate the number of occupied cells. (e–p) Values averaged over replicates (n = 3) and within each geological time step (95% CI given as thin lines for range filling and species richness)

high selective pressure to cope with competition. Because differentiated endemics did not change their niche upon speciation, their range filling dynamics were comparable to non-endemics.

The scenario without competition between non-endemics revealed similar trends but with higher values than the full model, suggesting that competition decreased the average range filling of non-endemics at intermediate island ages in the full model (compare Figure 6e with Figure 3b). The result that the average range filling was lower for radiated endemics was expected because these species still competed (see Section 2.13). These changes in the range filling indicated that competition regulated range dynamics (see also Cabral & Kreft, 2012; Urban et al., 2016). This regulation interacted with speciation and metabolic constraints, as endemic species could outcompete non-endemics. Indeed, without speciation, the range filling of non-endemics was always close to 100% (Figure 6h). However, without metabolic constraints there was complete absence of non-endemics at the end of our simulations (Figure 6f). The integration of other biotic interactions should alter range filling in more complex ways, as the interplay between mutualists and antagonists generates complex spatial patterns of occurrence (e.g. Kubisch, Holt, Poethke, & Fronhofer, 2014).

4.3 | Community level

In the full model, the general lognormal shape of the rank-abundance plots with few dominant species (Figure 4a) was consistent with an extensive empirical meta-analysis (Ulrich, Ollik, & Ugland, 2010). Moreover, species abundance distributions followed the recently proposed statistical distribution 'gambin' (Figure S5 of Appendix S2), which adequately describes species abundance distributions (Matthews et al., 2014). The spatio-temporal functional dynamics are consistent with empirical patterns, such as selection towards larger plants and loss of long-distance dispersal ability (Figure 4g,h; Cox & Burns, 2017; Whittaker & Fernández-Palacios, 2007). A previous modelling study showed that the realized trait structure along an elevational gradient can diverge from the initial random community, indicating there is selective pressure on trait compositions (Cabral & Kreft, 2012). Hence, our findings support empirical and theoretical evidence that dispersal might be lost in isolated habitats and on islands (Bonte et al., 2012; Cody & Overton, 1996). Future experiments could focus on functional and non-functional evolution and may improve our understanding of trait changes of insular species.

When assessing the spatial distribution of species richness, the mid-elevation peaks (Figure 4b,c) reflected the random distribution of temperature niches of the source pool, with most ranges overlapping in mid-elevations due to mid-domain effects (Cabral & Kreft, 2012; Colwell & Lees, 2000). Ignoring the ecotones, the percentage of radiated endemics was highest at lower elevations (Figure 4d). On real-world mountains, species richness often peaks at low elevations (Sanders & Rahbek, 2012). However, the percentage of single-island endemics tends to peak at high elevations (Steinbauer, Otto, Naranjo-Cigala, Beierkuhnlein, & Fernández-Palacios, 2012), which might be caused by higher isolation, lower competition and lower gene flow between high-elevation environments (Lomolino, 2001; Steinbauer et al., 2012), as well as due to human-induced loss of species in lowlands (Lomolino, 2001; Nogués-Bravo, Araújo, Romdal, & Rahbek, 2008). In our simulations, intermediate elevations were the least isolated environments, including a tendency to have high colonization rates, particularly compared to highlands (Figure S6 of Appendix S2). On the one hand, the higher proportion of both total and radiated endemics in the lowlands supports the isolation effects because these elevations were the most isolated. On the other hand, the low proportion of endemics at high elevations might reflect time and area effects, because high elevations had the smallest area and less time to accumulate species. Indeed, the scenario without environmental dynamics had a high proportion of radiated endemics at both low and high elevations (Figure 6k). Future experiments assessing richness gradients should focus on disentangling the role of temporal environmental availability from isolation to source pool.

Furthermore, environmental variables also affected endemism by increasing mutation and speciation rates with temperature (Allen, Gillooly, Savage, & Brown, 2006; Brown et al., 2004). Comparing the scenario without metabolic constraints and trade-offs between demographic rates to the full scenario (Figure 6j) indicated that metabolic constraints and trade-offs influenced the spatial structure of speciation and of local communities. Ignoring such constraints and trade-offs led to the evolution of super-dominant species (e.g. high survival rates and low resource requirements – Savage et al., 2004). Moreover, metabolic constraints interacted with competition to regulate optimal environments for speciation, indicated by the mid-elevation peaks in endemic richness at maximum island size in the full model (Figure 4c). This happens because metabolic constraints should generate higher speciation rates in the lowlands due to higher mutation rates, but should also generate stronger competition via higher resource requirements and thus lower carrying capacities (Allen et al., 2006; Brown et al., 2004). Consequently, mid-elevations represent the best balance between higher mutation rates and area availability in the lowlands versus lower competition pressure in the highlands. This provides an eco-evolutionary explanation of the common biodiversity peaks at mid-elevation (e.g. Nogués-Bravo et al., 2008).

4.4 | Assemblage level

Species richness of entire islands closely tracked environmental dynamics (Figure 5a,b). Slope values of power-law SARs were within the range of oceanic islands (mean z = 0.39 in Figure 5b compared to z = 0.38 in Triantis, Guilhaumon, & Whittaker, 2012). Moreover, the SAR intercepts reflecting the average species density (mean c = 1.4, Figure 5b) were comparable to intercepts reported for plants (c = 1.6 in Triantis et al., 2012), but larger than intercepts reported for oceanic islands (c = 0.6; Triantis et al., 2012). Such low reported intercepts are, nevertheless, closer to the intercepts obtained for the growth phase only (c = 0.55; Figure 5b). In the real world, low intercepts (i.e. low richness per unit area) are found for area-demanding taxa (e.g. vertebrates and trees) and for remote, very small and/or low-lying islands, such as atolls. These islands are also subject to frequent disturbances (Morrison, 2010), which were not simulated. The obtained differences in SARs indicate that future studies should account for the geological phase of the islands.

Species richness and endemic richness (Figure 5c) followed the humped temporal trend predicted by the GDM (Borregaard et al., 2016; Hortal, Roura-Pascual, Sanders, & Rahbek, 2010; Whittaker et al., 2008), even when varying geological trajectories (Figure S2 of Appendix S2). This hump was, however, absent in the scenario without environmental dynamics (Figure 6o), suggesting that the environmental processes drive the temporal dynamics of species richness. Changes in biogeographical patterns with island ontogeny were also previously reported (reviewed in Borregaard et al., 2016). Moreover, without environmental processes, species richness was stable (Figure 6o) and this is in line with the equilibrium theory of island biogeography's (ETIB) assumption of static islands (MacArthur & Wilson, 1963). Without ecological and evolutionary processes, the humped trend was retained, but richness values were affected (Figure 6m,n,p). In fact, species richness remained very low without metabolic constraints (Figure 6n) or reached high values without competition (Figure 6m). In both scenarios, island floras were dominated by endemics, suggesting that local competition and metabolic

constraints scale up to assemblage scales by affecting evolutionary processes and species coexistence (see also Pedersen, Sandel, & Svenning, 2014; Waters, Fraser, & Hewitt, 2013).

The proportion of endemic species increased over time (Figure 5d) and was mostly driven by mainland-island differentiation (Figure 3b). These trends diverged from an expected humped temporal trend (Whittaker et al., 2008), which seems to be better matched only by endemism derived from within-island radiation (Figure 5d). However, dispersal of single-island endemics from older to younger islands within archipelagos would cause species to lose their status as single-island endemics and thus create the humped temporal trend (Borregaard et al., 2016). Moreover, as islands age and lose height, they may be increasingly characterized by homogeneous, disturbed, open and strand-line habitats (e.g. atolls). These habitats are dominated by widespread and disturbance-tolerant species. Future studies could simulate these archipelagic and disturbance conditions to better capture the late endemism decrease.

In the scenario without speciation, the temporal humped trend of species richness indicated that the humped richness can emerge through colonization and extinction dynamics alone and is mostly driven by environmental dynamics as discussed above. In the full model, colonization and within-island radiation rates, nevertheless, followed the expected humped colonization and speciation rates (Figure 5e,f; Borregaard et al., 2016). Moreover, the humped trend of radiating lineages and species per radiating lineage (Figure 5g), of extinction rate (Figure 5e) and of mainland-island differentiation rate (Figure 5f) also followed GDM predictions (Borregaard et al., 2016; Cabral et al., 2019). Additionally, the variable temporal trends in species richness when looking at single lineages (Figure 5h,i) further reconciled our theoretical framework with empirical patterns diverging from the humped trend (Gillespie & Baldwin, 2010). Biogeographical rates did not reach a dynamic equilibrium. In fact, species accumulation dominated the growth phase whereas species extinction dominated the erosion phase (Figure 5e,f). While both ETIB and GDM do not distinguish the different modes of extinction, our results showed a noteworthy difference between local extinctions versus extinction of endemic species. The much more delayed peak in extinction rate of endemic species (compare Figure 5e,f) suggests that endemics were less susceptible to extinction than non-endemics.

Trait richness followed the humped trend of species richness, consistent with the reported positive relationship between trait and species richness (Figure 5c,j; Carnicer, Brotons, Stefanescu, & Penuelas, 2012; Petchey & Gaston, 2002). The initial high species packing followed by a sharp decrease (Figure 5k) possibly reflected strong environmental filtering (e.g. selecting for lowland-adapted, good dispersing herbs). With increasing environmental heterogeneity, new colonizers and evolving endemics increased the trait space, causing the decrease in species packing (Figure 5j). Thereafter, species start to pack the trait space, closely tracking island area. However, species packing was not random, as radiated endemics were selected to fill the environmental space away from the co-occurring island species thereby avoiding niche overlap and competitive exclusion (Mizera & Meszéna, 2003), while keeping some levels of similarity to ancestral species (Figure 5l) even if environmental preferences were not subject to phylogenetic constraints. While these results provide the mechanistic explanation of how isolation effects drive endemism via radiation of local flora, it also indicates complex interactions between trait, demographic and radiation dynamics (see Carnicer et al., 2012 for a review) and a strong influence of competition on trait evolution.

4.5 | Model properties, limitations and potentials

The ability of the model to simultaneously generate multiple patterns across different ecological levels provides opportunities for cross-scale validation (Grimm & Railsback, 2012). Other process-based island models (Borregaard et al., 2016; Hortal, Triantis, Meiri, Thebault, & Sfenthourakis, 2009; Kadmon & Allouche, 2007; Rosindell & Harmon, 2013; Rosindell & Phillimore, 2011; Valente, Etienne, & Phillimore, 2014; Valente, Phillimore, & Etienne, 2015) have fewer parameters and thus lower complexity. However, these models tend to simulate colonization, extinction and speciation directly and are spatially implicit. In BioGEEM these biogeographical processes emerge from low-level, population-level processes. Additionally, our explicit representation of space facilitates a niche-based framework, which is particularly relevant for island biogeography given the role of habitat heterogeneity and niche opportunities for speciation (Whittaker et al., 2008). Promising future model extensions might include microevolutionary components such as explicit population genetics (as also suggested by Schurr et al., 2012) or individual genomes (Schiffers, Bourne, Lavergne, Thuiller, & Travis, 2013), leading to more gradual trait divergences. While genetically explicit models should become gradually more computationally feasible, trait divergence upon point-mutation combined with protracted speciation proved already effective to generate lineage radiation.

Limited availability of empirical data hampers model validation, parameterization and quantification of model uncertainty (Dormann et al., 2012; Jeltsch, Moloney, Schurr, Köchy, & Schwager, 2008). The hierarchical structure of BioGEEM allows to calibrate the model and to evaluate emergent patterns with different data types (Wiegand, Jeltsch, Hanski, & Grimm, 2003). For example, estimates of demographic rates could be used to fit metabolic functions (Schurr et al., 2012) and abundance distributions to fit demographic functions (Cabral & Schurr, 2010). Simulating large, species-rich ecosystems might still be a computational challenge, but data scarcity can be overcome with pattern-oriented modelling to calibrate unknown parameters and prevent error propagation (Grimm & Railsback, 2012; Wiegand et al., 2003). Moreover, the insights gained with explorative experiments switching off processes demonstrated that this should be done more often in modelling studies.

We used empirical data and theoretical predictions for model evaluation. A range of emergent patterns followed well-documented empirical trends and relationships. Namely, these were rank-abundance distributions (Ulrich et al., 2010), relationships

between proportions of endemic species and environmental isolation (Steinbauer et al., 2012), SARs (Triantis et al., 2012) and species richness and endemism over time (Cameron et al., 2013; Whittaker et al., 2008). Such cross-pattern validation suggests that BioGEEM is generalizable across ecological levels (see Evans et al., 2013 for generality of complex models). This is unprecedented, as previous island models focus on processes and patterns at only one or two ecological levels (Leidinger & Cabral, 2017). Some of the emergent patterns lack empirical data for evaluation and thus constitute predictions to be tested in future studies (e.g. humped trait diversity over time, Figure 5j). Additionally, BioGEEM integrates inherent variability in demographic, colonization, extinction and speciation rates. Finally, parameter and model uncertainties can be addressed by varying scenarios (e.g. different isolation scenarios – Cabral et al., 2019) and model structure (Figure 6). Therefore, data limitation should not prevent the further exploration of biodiversity dynamics.

4.6 | Theoretical implications and conclusions

Our experiments showed that a realistic representation of biodiversity dynamics requires the simultaneous consideration of multiple ecological, evolutionary and environmental processes. Unrealistic patterns emerged when switching off processes that were based on distinct ecological theories. Developing a multi-theoretical model is not trivial and could here be achieved by simulating individual- and population-level processes in a stochastic, niche-based and metabolic framework. Patterns at these ecological levels scale up and lead to biogeographical dynamics that mechanistically link low-level (coexistence and metabolic theory) with high-level theories (island biogeography). We can gain insights from this theory integration. For example, the metabolic theory predicts higher speciation rates in higher temperatures, but the obtained higher endemism in more isolated habitats (including those with low temperatures) indicated important interactions between metabolic constraints and competition. Moreover, extinction rates vary between non-endemic and endemic species and endemism may increase steadily. Although, these results are yet to be contrasted against field data, they demonstrate the explorative potential of theoretically integrative models. We further argue that such models constitute 'virtual, long-term field stations' integrating biogeography and macroecology to other fields of ecology and generalizing findings across ecological levels. These models can thus be used to study specific drivers and patterns (e.g. isolation effects on biogeographical patterns – Cabral et al.,2019) or particular systems (oceanic islands, fragments, continuous habitat).

ACKNOWLEDGEMENTS

J.S.C. acknowledges funding from the sDiv, the Synthesis Centre of iDiv (DFG FZT 118). H.K. was supported by the DFG through the German Excellence Initiative. K.W. was partly funded by the State of Lower Saxony (Ministry of Science and Culture; Cluster of Excellence 'Functional Biodiversity Research'). We thank Albert Phillimore, James Rosindell, Kostas Triantis, Robert Whittaker, Yael Kisel, Gunnar Petter, Anke Stein, Patrick Weigelt, Carsten Meyer, Adam Anderson, Joanne Bennett, the editors Brent Emerson and Michael Dawson and three anonymous reviewers for comments.

ORCID

Juliano Sarmento Cabral https://orcid.org/0000-0002-0116-220X
Kerstin Wiegand https://orcid.org/0000-0003-4854-0607
Holger Kreft https://orcid.org/0000-0003-4471-8236

REFERENCES

Allen, A. P., Gillooly, J. F., Savage, V. M., & Brown, J. H. (2006). Kinetic effects of temperature on rates of genetic divergence and speciation. *Proceedings of the National Academy of Sciences of the United States of America*, *103*, 9130–9135.

Bonte, D., Van Dyck, H., Bullock, J. M., Coulon, A., Delgado, M., Gibbs, M., … Travis, J. M. J. (2012). Costs of dispersal. *Biological Reviews*, *87*, 290–312.

Borregaard, M. K., Matthews, T. J., & Whittaker, R. J. (2016). The general dynamic model: Towards a unified theory of island biogeography? *Global Ecology and Biogeography*, *25*, 85–816.

Brown, J. H., Gillooly, J. F., Allen, A. P., Savage, V. M., & West, G. B. (2004). Toward a metabolic theory of ecology. *Ecology*, *85*, 1771–1789.

Cabral, J. S., & Kreft, H. (2012). Linking ecological niche, community ecology and biogeography: Insights from a mechanistic niche model. *Journal of Biogeography*, *39*, 2212–2224.

Cabral, J. S., & Schurr, F. M. (2010). Estimating demographic models for the range dynamics of plant species. *Global Ecology and Biogeography*, *19*, 85–97.

Cabral, J. S., Valente, L., & Hartig, F. (2017). Mechanistic models in macroecology and biogeography: State-of-art and prospects. *Ecography*, *40*, 267–280.

Cabral, J. S., Whittaker, R. J., Wiegand, K., & Kreft, H. (2019). Assessing predicted isolation effects from the general dynamic model of island biogeography with an eco-evolutionary model for plants. *Journal of Biogeography*, 1–13.

Cameron, R. A. D., Triantis, K. A., Parent, C. E., Guilhaumon, F., Alonso, M. R., Ibáñez, M., … Whittaker, R. J. (2013). Snails on oceanic islands: Testing the general dynamic model of oceanic island biogeography using linear mixed effect models. *Journal of Biogeography*, *40*, 117–130.

Carnicer, J., Brotons, L., Stefanescu, C., & Penuelas, J. (2012). Biogeography of species richness gradients: Linking adaptive traits, demography and diversification. *Biological Reviews*, *87*, 457–479.

Clark, J. S., Silman, M., Kern, R., Macklin, E., & HilleRisLambers, J. (1999). Seed dispersal near and far: Patterns across temperate and tropical forests. *Ecology*, *80*, 1475–1494.

Cody, M. L., & Overton, J. M. C. (1996). Short-term evolution of reduced dispersal in island plant populations. *Journal of Ecology*, *84*, 53–61.

Colwell, R. K., & Lees, D. C. (2000). The mid-domain effect: Geometric constraints on the geography of species richness. *Trends in Ecology & Evolution*, *15*, 70–76.

Colwell, R. K., & Rangel, T. F. (2010). A stochastic, evolutionary model for range shifts and richness on tropical elevational gradients under Quaternary glacial cycles. *Philosophical Transactions of the Royal Society B-Biological Sciences*, *365*, 3695–3707.

Cox, B. T. M., & Burns, K. C. (2017). Convergent evolution of gigantism in the flora of an isolated archipelago. *Evolutionary Ecology*, *31*, 741–752.

Chesson, P. (2000). Mechanisms of maintenance of species diversity. *Annual review of Ecology and Systematics*, *31*, 343–366.

Darwin, C. (1859). *On the Origin of Species by Means of Natural Selection*.London, UK:J. Murray.

Dormann, C. F., Schymanski, S. J., Cabral, J., Chuine, I., Graham, C., Hartig, F., … Schröder, B. (2012). Correlation and process in species distribution models: Bridging a dichotomy. *Journal of Biogeography*, *39*, 2119–2131.

Emerson, B. C., & Patiño, J. (2018a). Anagenesis, cladogenesis, and speciation on islands. *Trends in Ecology & Evolution*, *33*, 488–391.

Emerson, B. C., & Patiño, J. (2018b). Babies, bathwater, and straw men? Not quite: a response to Meiri et al. *Trends in Ecology & Evolution*, *33*, 896–897.

Evans, M. R., Grimm, V., Johst, K., Knuuttila, T., de Langhe, R., Lessells, C. M., … Weisberg, M. (2013). Do simple models lead to generality in ecology? *Trends in Ecology & Evolution*, *28*, 578–583.

Gillespie, R. G., & Baldwin, B. G. (2010). Island biogeography of remote archipelagoes. In J. B. Losos & R. E. Ricklefs (Eds.), *The theory of island biogeography revisited* (pp. 358–387). Princeton, NJ: Princeton University Press.

Gotelli, N. J., Anderson, M. J., Arita, H. T., Chao, A., Colwell, R. K., Connolly, S. R., … Willig, M. R. (2009). Patterns and causes of species richness: A general simulation model for macroecology. *Ecology Letters*, *12*, 873–886.

Grimm, V., Berger, U., DeAngelis, D. L., Polhill, J. G., Giske, J., & Railsback, S. F. (2010). The ODD protocol A review and first update. *Ecological Modelling*, *221*, 2760–2768.

Grimm, V., & Railsback, S. F. (2012). Pattern-oriented modelling: A 'multi-scope' for predictive systems ecology. *Philosophical Transactions of the Royal Society B: Biological Sciences*, *367*, 298–310.

Hanski, I. (1999). *Metapopulation ecology*. Oxford, UK: Oxford University Press.

Harfoot, M. B., Newbold, T., Tittensor, D. P., Emmott, S., Hutton, J., Lyutsarev, V., … Purves, D. W. (2014). Emergent global patterns of ecosystem structure and function from a mechanistic general ecosystem model. *PLoS Biology*, *12*, e1001841.

Hortal, J., Roura-Pascual, N., Sanders, N. J., & Rahbek, C. (2010). Understanding (insect) species distributions across spatial scales. *Ecography*, *33*, 51–53.

Hortal, J., Triantis, K. A., Meiri, S., Thebault, E., & Sfenthourakis, S. (2009). Island species richness increases with habitat diversity. *American Naturalist*, *174*, E205–E217.

Hurlbert, A. H., & Stegen, J. C. (2014). On the processes generating latitudinal richness gradients: Identifying diagnostic patterns and predictions. *Frontiers in Genetics*, *5*, 420.

Jeltsch, F., Moloney, K. A., Schurr, F. M., Köchy, M., & Schwager, M. (2008). The state of plant population modelling in light of environmental change. *Perspectives in Plant Ecology, Evolution and Systematics*, *9*, 171–189.

Kadmon, R., & Allouche, O. (2007). Integrating the effects of area, isolation, and habitat heterogeneity on species diversity: A unification of island biogeography and niche theory. *The American Naturalist*, *170*, 443–454.

Kisel, Y., & Barraclough, T. G. (2010). Speciation has a spatial scale that depends on levels of gene flow. *The American Naturalist*, *175*, 316–334.

Kissling, W. D., Dormann, C. F., Groeneveld, J., Hickler, T., Kühn, I., McInerny, G. J., … Schurr, F. M. (2012). Towards novel approaches to modelling biotic interactions in multispecies assemblages at large spatial extents. *Journal of Biogeography*, *39*, 2163–2178.

Kubisch, A., Holt, R. D., Poethke, H. J., & Fronhofer, E. A. (2014). Where am I and why? Synthesizing range biology and the eco-evolutionary dynamics of dispersal. *Oikos*, *123*, 5–22.

Kueffer, C., Daehler, C. C., Torres-Santana, C. W., Lavergne, C., Meyer, J.-Y., Otto, R., & Silva, L. (2010). A global comparison of plant invasions on oceanic islands. *Perspectives in Plant Ecology, Evolution and Systematics*, *12*, 145–161.

Leidinger, L., & Cabral, J. S. (2017). Biodiversity dynamics on islands: Explicitly accounting for causality in mechanistic models. *Diversity*, *9*, 30.

Lomolino, M. (2001). Elevational gradients of species-density: Historical and prospective views. *Global Ecology and Biogeography*, *10*, 3–13.

Losos, J. B., & Ricklefs, R. E. (2010). *The theory of island biogeography revisited*. Princeton, NJ: Princeton University Press.

MacArthur, R. H., & Wilson, E. O. (1963). An equilibrium theory of insular zoogeography. *Evolution*, *17*, 373–387.

Matthews, T. J., Borregaard, M. K., Ugland, K. I., Borges, P. A. V., Rigal, F., Cardoso, P., & Whittaker, R. J. (2014). The gambin model provides a superior fit to species abundance distributions with a single free parameter: Evidence, implementation and interpretation. *Ecography*, *37*, 1002–1011.

McGill, B. J. (2012). Trees are rarely most abundant where they grow best. *Journal of Plant Ecology*, *5*, 46–51.

Meiri, S., Raia, P., & Santos, A. M. (2018). Anagenesis and cladogenesis are useful island biogeography terms. *Trends in Ecology & Evolution*, *33*, 895–896.

Mizera, F., & Meszéna, G. (2003). Spatial niche packing, character displacement and adaptive speciation along an environmental gradient. *Evolutionary Ecology Research*, *5*, 363–382.

Morrison, L. W. (2010). Long-term non-equilibrium dynamics of insular floras: A 17-year record. *Global Ecology and Biogeography*, *19*, 663–672.

Murray, K., & Conner, M. M. (2009). Methods to quantify variable importance: Implications for the analysis of noisy ecological data. *Ecology*, *90*, 348–355.

Nathan, R., & Muller-Landau, H. C. (2000). Spatial patterns of seed dispersal, their determinants and consequences for recruitment. *Trends in Ecology & Evolution*, *15*, 278–285.

Nogués-Bravo, D., Araújo, M. B., Romdal, T., & Rahbek, C. (2008). Scale effects and human impact on the elevational species richness gradients. *Nature*, *453*, 216–220.

Olesen, J. M., Eskildsen, L. I., & Venkatasamy, S. (2002). Invasion of pollination networks on oceanic islands: Importance of invader complexes and endemic super generalists. *Diversity and Distributions*, *8*, 181–192.

Pedersen, R. Ø., Sandel, B., & Svenning, J.-C. (2014). Macroecological evidence for competitive regional-scale interactions between the two major clades of mammal carnivores (Feliformia and Caniformia). *PLoS ONE*, *9*, e100553.

Petchey, O. L., & Gaston, K. J. (2002). Functional diversity (FD), species richness and community composition. *Ecology Letters*, *5*, 402–411.

Pontarp, M., Bunnefeld, L., Cabral, J. S., Etienne, R. S., Fritz, S. A., Gillespie, R., … Jansson, R. (2019). The latitudinal diversity gradient: Novel understanding through mechanistic eco-evolutionary models. *Trends in Ecology & Evolution*, *34*,211-223early view.

R Core Team. (2018). *R: A language and environment for statistical computing*. Vienna, Austria: R Foundation for Statistical Computing. http://www.R-project.org/

Rangel, T. F., Edwards, N. R., Holden, P. B., Diniz-Filho, J. A. F., Gosling, W. D., Coelho, M. T. P., … Colwell, R. K. (2018). Modeling the ecology and evolution of biodiversity: Biogeographical cradles, museums, and graves. *Science*, *361*, eaar5452.

Ricklefs, R. E., & Bermingham, E. (2004). History and the species-area relationship in Lesser Antillean birds. *American Naturalist*, *163*, 227–239.

Rosindell, J., & Harmon, L. J. (2013). A unified model of species immigration, extinction and abundance on islands. *Journal of Biogeography*, *40*, 1107–1118.

Rosindell, J., & Phillimore, A. B. (2011). A unified model of island biogeography sheds light on the zone of radiation. *Ecology Letters*, *14*, 552–560.

Sanders, N. J., & Rahbek, C. (2012). The patterns and causes of elevational diversity gradients. *Ecography*, *35*, 1.

Sanderson, C., & Curtin, R. (2016). Armadillo: A template-based C++ library for linear algebra. *Journal of Open Source Software*, *1*, 26.

Savage, V. M., Gillooly, J. E., Brown, J. H., West, G. B., & Charnov, E. L. (2004). Effects of body size and temperature on population growth. *The American Naturalist*, *163*, 429–441.

Schiffers, K., Bourne, E. C., Lavergne, S., Thuiller, W., & Travis, J. M. (2013). Limited evolutionary rescue of locally adapted populations facing climate change. *Philosophical Transactions of the Royal Society of London B: Biological Sciences*, *368*, 20120083.

Schurr, F. M., Pagel, J., Cabral, J. S., Groeneveld, J., Bykova, O., O'Hara, R. B., … Midgley, G. F. (2012). How to understand species' niches and range dynamics: A demographic research agenda for biogeography. *Journal of Biogeography*, *39*, 2146–2162.

Steinbauer, M. J., Otto, R., Naranjo-Cigala, A., Beierkuhnlein, C., & Fernández-Palacios, J. M. (2012). Increase of island endemism with altitude–speciation processes on oceanic islands. *Ecography*, *35*, 23–32.

Stuessy, T. F., Jakubowsky, G., Gómez, R. S., Pfosser, M., Schlüter, P. M., Fer, T., … Kato, H. (2006). Anagenetic evolution in island plants. *Journal of Biogeography*, *33*, 1259–1265.

Triantis, K. A., Guilhaumon, F., & Whittaker, R. J. (2012). The island species–area relationship: Biology and statistics. *Journal of Biogeography*, *39*, 215–231.

Ulrich, W., Ollik, M., & Ugland, K. I. (2010). A meta-analysis of species–abundance distributions. *Oikos*, *119*, 1149–1155.

Urban, M. C., Bocedi, G., Hendry, A. P., Mihoub, J. B., Pe'er, G., Singer, A.… Travis, J. M. (2016). Improving the forecast for biodiversity under climate change. *Science*, *353*, aad8466.

Valente, L. M., Etienne, R. S., & Phillimore, A. B. (2014). The effects of island ontogeny on species diversity and phylogeny. *Proceedings of the Royal Society of London B: Biological Sciences*, *281*, 20133227.

Valente, L. M., Phillimore, A. B., & Etienne, R. S. (2015). Equilibrium and non-equilibrium dynamics simultaneously operate in the Galápagos islands. *Ecology Letters*, *18*, 844–852.

Warren, B. H., Simberloff, D., Ricklefs, R. E., Aguilée, R., Condamine, F. L., Gravel, D., … Thébaud, C. (2015). Islands as model systems in ecology and evolution: Prospects fifty years after MacArthur-Wilson. *Ecology Letters*, *18*, 200–217.

Waters, J. M., Fraser, C. I., & Hewitt, G. M. (2013). Founder takes all: Density-dependent processes structure biodiversity. *Trends in Ecology & Evolution*, *28*, 78–85.

Weigelt, P., Steinbauer, M. J., Cabral, J. S., & Kreft, H. (2016). Late Quaternary climate change shapes island biodiversity. *Nature*, *532*, 99–102.

White, J. W., Rassweiler, A., Samhouri, J. F., Stier, A. C., & White, C. (2014). Ecologists should not use statistical significance tests to interpret simulation model results. *Oikos*, *123*, 385–388.

Whittaker, R. J., & Fernández-Palacios, J. M. (2007). *Island biogeography: Ecology, evolution, and conservation* (2nd ed). Oxford, UK: Oxford University Press.

Whittaker, R. J., Triantis, K. A., & Ladle, R. J. (2008). A general dynamic theory of oceanic island biogeography. *Journal of Biogeography*, *35*, 977–994.

Wiegand, K., Saltz, D., Ward, D., & Levin, S. A. (2008). The role of size inequality in self-thinning: A pattern-oriented simulation model for arid savannas. *Ecological Modelling*, *210*, 431–445.

Wiegand, T., Jeltsch, F., Hanski, I., & Grimm, V. (2003). Using pattern-oriented modeling for revealing hidden information: A key for reconciling ecological theory and application. *Oikos*, *100*, 209–222.

Wisz, M. S., Pottier, J., Kissling, W. D., Pellissier, L., Lenoir, J., Damgaard, C. F., … Guisan, A. (2013). The role of biotic interactions in shaping distributions and realised assemblages of species: Implications for species distribution modelling. *Biological Reviews*, *88*, 15–30.

BIOSKETCH

Juliano Sarmento Cabral is interested in processes and factors influencing species and biodiversity dynamics across spatio-temporal scales. His research includes processes determining spatial and temporal distribution of tropical epiphytes, species ranges, island plant diversity as well as global species richness and endemism patterns.

Kerstin Wiegand is interested in the role of space for population dynamics, interspecific interactions and biodiversity. The methodological emphasis of her research is on (spatially explicit, agent-based) simulation models and spatial statistics.

Holger Kreft has a broad interest in biogeographical and macroecological patterns, particularly gradients in species richness and endemism. His research includes analyses of plant and vertebrate diversity, island and conservation biogeography.

Author contributions: J.S.C. and H.K. designed the study, with input from K.W.; J.S.C. implemented the model and simulated the experiments; J.S.C. led the analyses and writing, with input from all co-authors.

SUPPORTING INFORMATION

Additional supporting information may be found online in the Supporting Information section at the end of the article.

How to cite this article: Cabral JS, Wiegand K, Kreft H. Interactions between ecological, evolutionary and environmental processes unveil complex dynamics of insular plant diversity. *J Biogeogr*. 2019;46:1582–1597. https://doi.org/10.1111/jbi.13606